Endocycles support tissue growth and regeneration of the adult Drosophila accessory gland

Allison M. Box[1], Samuel Jaimian Church[1], Shyama Nandakumar[1], Dilan Prasad[1], Ariana Afrakhteh[1], Russell S. Taichman[2], and Laura Buttitta[1]

[1] Department of Molecular, Cellular and Developmental Biology, University of Michigan, Ann Arbor, MI 48109, USA

[2] Department of Periodontology, School of Dentistry, University of Alabama at Birmingham, Birmingham, AL

* Author for correspondence: buttitta@umich.edu

Abstract

The *Drosophila melanogaster* male accessory gland is a functional analog of the mammalian prostate containing two secretory epithelial cell types, termed main and secondary cells. This tissue is responsible for making and secreting seminal fluid proteins and other molecules that contribute to successful reproduction. Here we show that similar to the mammalian prostate, this tissue grows with age and can undergo functional regeneration post-damage. We describe a post-eclosion endocycle required for gland maturation, that is dependent on juvenile hormone signaling. In addition, the differentiated binucleated main cells of the adult accessory gland continue to undergo rare endocycles throughout physiological aging to increase DNA content and cell size. Accessory gland cells remain poised to endocycle and upregulation of signals that promote endocycling and tissue growth are sufficient to trigger dramatic increases in cell ploidy. We provide evidence that the main cells of this tissue remain poised to enter the endocycle to assist in tissue regrowth after damage, providing a novel model for postmitotic regeneration in a binucleate tissue.

Introduction

The *Drosophila* male accessory gland is functionally analogous to the mammalian prostate. This organ is an essential component of the male reproductive system and is responsible for making and secreting seminal fluid proteins, sex peptides, and anti-microbial proteins that are transferred to the female upon mating (Adams & Wolfner, 2007; Heifetz, Vandenberg, Cohn, & Wolfner, 2005; Lung, Kuo, & Wolfner, 2001; Qazi & Wolfner, 2003; Ravi Ram, Ji, & Wolfner, 2005). The bi-lobed accessory gland consists of a single layer of secretory epithelial cells that form a large lumen apically and are surrounded basally by extracellular matrix and a muscle layer (Bairati, 1968; Susic-Jung et al., 2012). Each lobe of the accessory gland consists of approximately 1,000 binucleate and polyploid epithelial cells, which are made up of two cell types: main cells and secondary cells (Bairati, 1968). Main cells are the smaller of the two types and are hexagonal in shape. These cells make up a majority of the gland and are located predominantly in the proximal and medial portions of the lobes. Secondary cells are larger, more luminal cells that are located at the distal tip of the lobes. There are approximately 40-60 secondary cells in each lobe, with the rest of the cells (~940-960 cells) being main cells. Main and secondary cells have distinct but partially overlapping secretory protein profiles, and both cell types play an important role in fecundity(Bertram, Akerkar, Ard, Gonzalez, & Wolfner, 1992; Sitnik, Gligorov, Maeda, Karch, & Wolfner, 2016).

Accessory gland development takes place during larval and pupal stages and involves developmental cell cycle regulation that includes variant cell cycles. In late larval stages, FGF signaling drives recruitment of mesodermal cells to the genital disc. These cells undergo a mesenchymal to epithelial transition and give rise to the precursors for the accessory glands and seminal vesicles (Ahmad & Baker, 2002). During early metamorphosis, the accessory gland progenitors increase in number by standard mitotic cell cycles. Approximately 50-55 hours after pupa formation, the cells of the developing accessory gland arrest proliferation and synchronously enter a truncated, variant cell cycle, in which nuclear division occurs but cytokinesis does not, resulting in the binucleation of the epithelial cells of the accessory gland. Approximately 10 hours later, the cells enter an additional synchronized endocycle, increasing their DNA content (C) without mitosis. This results in ~1,000 8C binucleated cells, each cell containing two 4C nuclei. It has been

previously reported that after the endocycle in the pupal stage, the cells of the accessory gland exit the cell cycle (Taniguchi et al., 2014). However more recent studies have shown that secondary cells retain the capacity to endocycle in response hormonal or mating signals (Leiblich et al., 2019) while main cells are thought to remain largely quiescent in the adult (Leiblich et al., 2019, 2012).

We examined the cell cycle status of main cells of the adult accessory gland starting immediately post-eclosion and find many examples of endoreplication, including a previously undescribed post-eclosion endocycle that requires juvenile hormone (JH) signaling. Induction of cell cycle and growth regulators are sufficient to trigger a dramatic increase of endocycling in the differentiated adult main cells, demonstrating that accessory gland cells remain poised to re-enter the cell cycle. We hypothesized that the main cells of the adult accessory gland remain poised to endocycle in order to maintain capacity for gland regeneration upon tissue damage. Indeed, the adult accessory gland is capable of functional regeneration after damage in part, due to increases in cell size and endocycling. Our findings establish a previously undescribed adult stage of accessory gland development and maturation and introduce the *Drosophila* accessory gland as a system to study factors underlying regeneration in a non-mitotic tissue.

The adult accessory gland grows via main cell endoreplication under normal physiological conditions throughout lifespan.

Like the mammalian prostate, the *Drosophila* accessory gland (AG) grows with age. AGs from virgin males undergo a period of rapid growth from the day of eclosion to day 10 post eclosion (Fig 1A), and continue to grow, albeit at a lesser rate throughout adulthood (Fig 1B). While a majority of AG growth in early adulthood can be attributed to the production and secretion of sex peptides, which expands the lumen of the gland and flattens the cells, we hypothesized that changes in cell number or cell size may also contribute to gland growth. To address whether changes in cell number contribute to gland growth, we stained the adult glands for the mitotic marker, phospho-histone H3 (PH3), at various time points throughout the male lifespan. In sum, over 100 glands, of various ages and mating status,

were negative for PH3 staining suggesting that under normal physiological conditions, gland growth is due to changes in cell size rather than cell number.

We next measured cell size for the major population of cells in the accessory gland, the main cells. Antibody staining for the septate junction protein Discs large (Dlg) was used to delineate epithelial cell-cell junctions for all cell size measurements. Cell size measurements reported here are not the full volume of a cell, but rather a measurement of the cell area at the level of the septate junctions. In virgin males, main cell area increases quickly with age and continues to increase throughout lifespan (Fig 1C). Additionally, the variation in main cell size also increases with age suggesting that a subset of main cells continue to grow. Because previous studies have established that cell size often scales with nuclear size and ploidy (Orr-Weaver, 2015), we next measured nuclear size in main cells across lifespan and found that nuclear area and variance also tracks with the increases in main cell size with age (Fig 1C). Together, our data shows a correlation between increased gland size, main cell size, and main cell nuclear area in virgin males throughout the lifespan of the fly.

Many *Drosophila* tissues undergo a variant cell cycle called an endocycle to increase cellular ploidy and tissue size in the absence of mitosis under normal physiological conditions (Edgar, Zielke, & Gutierrez, 2014; Orr-Weaver, 2015). Endocycling occurs when cells cycle through G/S phase without entering an M phase, thereby increasing DNA content (C) of a cell, resulting in polyploidy. Increased ploidy can contribute to increased biosynthesis, as is the case with *Drosophila* nurse cells (Inge Øvrebø & Edgar, 2018; Orr-Weaver, 2015). In this context, it would make sense that continued endocycling may be essential for optimal function of the adult accessory gland, which is highly secretory and responsible for making large amounts of specific proteins and other molecules for transfer to the female upon mating (Prince et al., 2019; C. Wilson, Leiblich, Goberdhan, & Hamdy, 2017). Since cell size scales with DNA content in many *Drosophila* endocycling cells (Von Stetina, Frawley, Unhavaithaya, & Orr-Weaver, 2018), we next examined whether DNA replication occurs in the main cells of the adult accessory gland.

We first examined the gland immediately post-eclosion. To label S-phases during this early timeframe we incubated dissected tissues in Ringer's solution with 5-Ethynyl-2′-deoxyuridine (EdU) for one hour, since flies do not eat at this stage. We observed that

100% of glands exhibit extensive EdU labeling in a large fraction of the main cells, suggesting that the adult AG undergoes an early, relatively synchronous endocycle immediately post-eclosion (Fig 1D, Fig 1H, Supplement 1A). We believe this early endocycle in the adult gland has been previously missed due to the use of feeding-based labeling assays, since male flies do not eat for approximately 7-8 hours post eclosion. DAPI intensity measurements of accessory glands at 10 days confirm that DNA content for the majority of main cell nuclei are 8C (Fig 1G), thus the adult-stage endocycle results in cells that are 16C (with 2x8C nuclei). We hypothesize that this widespread endocycle acts as an additional developmental stage for the accessory gland that likely supports the extensive growth reported during the first few days of adulthood and tissue maturation.

To assess whether endocycling continues in aging adults, where gland growth continues at a much slower rate, we performed EdU incorporation experiments by feeding adult male flies an EdU+sucrose mixture for 10 day periods at different time points throughout their lifespan. This longer-term, feeding-based EdU labeling allows us to visualize slow or rare DNA replication events in the adult accessory gland. We find that a small fraction of main cells incorporate EdU throughout the lifespan of the fly, even up to 40-50 days of age, in more than 50% of glands (Fig 1D, Fig 1H, Fig 1I) EdU incorporation occurs under both starved and fed conditions (Supplement 1B). We compared DAPI intensity measurements from the EdU positive nuclei with those from the EdU negative nuclei and find the EdU positive population has ~1.7x more DAPI signal than the EdU negative population (Fig 1J). During our studies, we frequently observe EdU incorporation in the main cell population, however we only very rarely observed EdU labeling in secondary cells, in mated and unmated males (Fig 1E,F). Altogether, this data shows that most main cells undergo an endocycle shortly post-eclosion and subsets of cells may continue to endocycle throughout the *Drosophila* lifespan under normal, physiological conditions.

Cell cycle oscillations in the adult accessory gland

Our pulsed and long-term EdU labeling approaches provide a static picture of S-phase in the AG but does not reveal cell cycle transitions and oscillations in real-time. To address this, we used the fly FUCCI cell cycle reporter to examine the oscillations of the cell cycle

degradation machinery in the accessory gland (Norman Zielke et al., 2014). We used *Paired-Gal4* (*Prd-Gal4*), a driver that has been established to express in both main and secondary cells, to drive expression of the cell cycle protein degrons mRFP1-CycB$_{1–266}$, to assay APC/C^{Cdh1} activity, and GFP-E2F1$_{1–230}$, to assay CRL4(Cdt2) activity (Supplement 2A). We find that >24h post-eclosion, the majority of main and secondary cells have low levels of mRFP1-CycB$_{1–266}$ indicating most cells are normally in a Gap phase with high APC/C^{Cdh1} activity, except for a small subset of main cells and very rare secondary cells where high mRFP1-CycB$_{1–266}$ indicates low APC/C^{Cdh1} activity. The low APC/C^{Cdh1} activity in endocycles results from transient high CycE/Cdk2 which also triggers S-phase, suggesting these cells have recently undergone DNA synthesis (Narbonne-Reveau et al., 2008; Norman Zielke, Querings, Rottig, Lehner, & Sprenger, 2008). The relatively low numbers of these cells at individual fixed timepoints agrees with the rare S-phase labeling we observe in our longer term EdU feeding. The GFP-E2F1$_{1–230}$ reporter indicates CRL4(Cdt2) activity which is normally high during S-phase and low during Gap phase. The high levels of GFP-E2F1$_{1–230}$ throughout the gland verifies that most cells are in a Gap phase where CRL4(Cdt2) activity is low, but a number of main cells and rare secondary cells show high CRL4(Cdt2) activity, consistent with transitions through S-phase. This fly FUCCI signature is similar to other endocycling cells, such as the intestinal enterocytes (Norman Zielke et al., 2014).

We verified the Fly FUCCI results by using the RGB cell cycle sensor as an additional tool to track cell cycle degradation machinery activity (Supplement 2B). The RGB cell cycle sensor uses the Gal4-UAS system to drive overexpression of cell cycle protein degrons nlsCycB$^{1-96}$-nlsCycB$^{1-285}$-tdTomato, to assay APC/C activity, and nlsCdt1$^{1-101}$-EBFP2, to visualize CRL4(Cdt2) activity, as well as a full length EGFP-PCNA to visualize early S Phase (Handke, Szabad, Lidsky, Hafen, & Lehner, 2014). While similar in concept to Fly FUCCI, a few notable differences include: a different length fragment of CycB, the use of nlsCdt1$^{1-101}$ instead of E2F1$_{1–230}$, and the expression of all 3 fluorescent reporters from a single transcript. Consistent with our findings using Fly FUCCI, we see that generally APC/C activity is high and CRL4(Cdt2) activity is low throughout the gland with only a small subset of main cells exhibiting EGFP-PCNA foci indicative of S-Phase. Importantly, oscillations of the cell cycle degrons occur at the distal tip of the gland where main and

secondary cells are located, as well as mid-lobe where there are main cells (Supplement 2B).

One caveat of the cell cycle reporters is their dependence on the Gal4-UAS system for ectopic expression of fluorescently tagged degrons. We therefore confirmed our observations using an endogenously tagged PCNA (PCNA::GFP) to confirm the presence of PCNA protein and to use GFP expression as a real-time read out of S-phase activity in this tissue (Blythe & Wieschaus, 2016). PCNA::GFP is present in nearly every main cell on the day of eclosion, the timepoint that we report widespread EdU labeling (Supplement 2C). Consistent with our EdU labeling on the day of eclosion and fly FUCCI data, we see lower levels of PCNA::GFP in secondary cells than main cells.

The E2F/Rbf Network and APC/C oscillations are required for developmental endocycle in the early adult AG

To further characterize the endocycle that occurs shortly post-eclosion, we used *Prd-Gal4* to manipulate gene expression using RNAi and overexpression constructs to assess which cell cycle regulators may be important for achieving proper gland ploidy. In order to assess effects on endoreplication we used two experimental procedures; (1) a 1-hour labeling where dissected glands from males 0-3 hours post eclosion were incubated in Ringers with EdU to visualize changes in EdU incorporation and (2) DAPI fluorescence intensity measurements to analyze the resulting DNA content at day 10 post-eclosion. The combination of these experiments allows us to determine if a loss or increase of EdU on the day of eclosion represents a true loss or acceleration of the endocycle rather than a simply a delay in entry or slowing of the post-eclosion endocycle.

Previous work has established an important role for the E2F/Rb network in endocycling (Bosco, Du, & Orr-Weaver, 2001; Norman Zielke et al., 2011). In brief, the *Drosophila* E2f network consists of two E2Fs: E2f1, which is described to act as a transcriptional activator, and E2F2, which is described to act as a transcriptional repressor. DP is the common heterodimeric binding partner of both E2Fs. Most cycling and endocycling cells exhibit oscillatory E2F1 activity that increases transcription of genes that promote S-phase entry, including Cyclins and Cdks and factors that drive DNA synthesis, followed by S-phase dependent E2F1 degradation (Norman Zielke et al., 2011, Shibutani et

al). Rbf is an essential *Drosophila* ortholog of Retinoblastoma, which inhibits E2F activity and acts as a brake for E2F oscillations. This brake is released by phosphorylation and inactivation of Rbf by Cyclin D or Cyclin E paired with cyclin-dependent kinases.

We depleted Rbf in the accessory gland using RNAi and observed an increase of EdU incorporation on the day of eclosion as well increased DNA content at day 10, with nearly half of nuclei measuring 16C, making the overall DNA content of main cells 32C (Fig 2B, Fig 2D). This suggests Rbf acts in the adult gland to limit endocycling. To confirm this, we overexpressed Rbf280, a phospho-mutant version of Rbf that can no longer be inhibited by CycD or CycE -dependent kinase activity and therefore would be expected to block adult endocycles (Xin, Weng, Xu, & Du, 2002). Strikingly, overexpression of Rbf280 resulted in two distinct phenotypes in main cells. We saw decreased EdU incorporation shortly post-eclosion and nuclei with 4C DNA content, resulting in a majority of main cells with only 8C DNA content on day 10, suggesting that Rbf280 blocked the widespread endocycle as expected (Fig 2B, Fig 2E). However, Rbf280 overexpression also occasionally resulted in a second, unexpected phenotype with increased EdU labeling and DNA content at day 10, where a majority of nuclei contain 16C DNA content, resulting in 32C main cells (Supplement 3A, Fig 2E). Our data suggests that Rbf likely limits endocycling in the adult AG, however as we have observed in wings expressing Rbf280 (Flegel, Grushko, Bolin, Griggs, & Buttitta, 2016), there can be compensatory mechanisms that increase cell cycling when Rbf suppression of E2F activity hits a certain threshold. To confirm that Rbf acts to limit endocycling in adult glands, we overexpressed Cyclin D with its partner CDK4, that phosphorylates and inhibits endogenous Rbf in the accessory gland. We observed a widespread increase in S-phases on the day of eclosion (Fig 2B) and increased ploidies at day 10 with nuclei up to 32 C, resulting in bi-nucleate cells with DNA content up to 64C (Fig 2D).

We next examined the role of E2Fs, E2F1 and E2F2, in accessory gland main cell endocycling. When E2F1 RNAi is expressed throughout the gland, we found widespread, prolonged EdU incorporation on the day of eclosion (Fig 2B). The prolonged labeling without an obvious increase in nuclear size suggests that RNAi inhibition of E2F1 slows the endocycle on the day of eclosion but does not prevent it. Strikingly, when the AG was depleted of E2F2 via RNAi we found EdU incorporation on the day of eclosion was nearly

abolished in all animals analyzed (Fig 2B). To determine whether this negative staining result was a delay vs. suppression of the endocycle, DNA content of main cell nuclei was measured on day 10 and found to be only 4C (Fig 2E), suggesting that E2F2 may be necessary for the adult developmental endocycle on the day of eclosion. This result was further verified by DNA content measurements of E2F null mutant/deficiency males at day 10, which also show a dramatic loss of the 8C population (Fig 2E). Altogether our data show that the E2F/Rbf network is a critical regulator of proper endocycling in main cells, and reveals an unexpected role for E2F2 in either directly or indirectly promoting the endocycle in this tissue.

In addition to oscillations of E2F activity, oscillations of the Anaphase Promoting Complex/Cyclosome (APC/C) are also required for proper endocycle progression in other tissues like the ovary and salivary gland (Narbonne-Reveau et al., 2008). The APC/C is a ubiquitin ligase that targets many cell cycle proteins for destruction and in the endocycle APC/C activity oscillations are essential for degradation of the replication inhibitor Geminin (N. Zielke, Querings, Rottig, Lehner, & Sprenger, 2008).To determine whether inhibition of APC/C oscillations would also disrupt proper endocycling in the main cells, we overexpressed Regulator of Cyclin A1 (Rca1; in mammals Emil1), an inhibitor of APC/C activity, in the accessory gland. When we inhibit the APC/C, EdU labeling on the day of eclosion in suppressed (Fig 2C) and at day 10 most main cells have a nuclear DNA content of only 2C, resulting in bi-nucleate main cells with a DNA content as low 4C (Fig 2E). This suggests that blocking the APC/C effectively prevents the pupal endocycle as well as subsequent endocycles in the adult tissue. To confirm this, we also overexpressed CyclinE/Cdk2, which can act to inhibit APC/C activity and block the endocycle (N. Zielke et al., 2008). Indeed, overexpression of CycE/Cdk2 inhibited EdU labeling on the day of eclosion, although effects on nuclear size appeared milder than with Rca1 expression. Together our data suggests that the oscillations of E2F and APC/C activity are critical for proper endocycle progression in the *Drosophila* main cells, and that blocking the endocycle on the day of eclosion results in a failure of the gland to reach normal ploidies.

dMyc and juvenile hormone signaling are required for adult accessory gland endocycling and function

We next examined which growth regulators may act upstream of the endocycle oscillators to promote gland growth on the day of eclosion. Work in other post-mitotic adult tissues has shown the transcription factor dMyc and the transcriptional co-regulator for the Hippo pathway, Yorkie (Yki; in mammals Yap), to mediate increased ploidy in tissues (Maines, Stevens, Tong, & Stein, 2004; Pierce et al., 2004). We therefore tested the roles of Yki and Myc in promoting accessory gland endocycling.

We used *Prd-Gal4* driving RNAis to knock-down Yki or dMyc in the accessory gland. We first analyzed the wave of endocycling that occurs just hours post eclosion. We see that EdU incorporation on the day of eclosion seems unperturbed when knocking down Yki, but EdU incorporation is reduced when knocking down dMyc (Fig 3A). Glands depleted for dMyc until 10 days post-eclosion exhibited disrupted epithelial structure as shown by DLG staining and a decrease in nuclear DNA content, with the majority of nuclei 4C and in the most severe case, as low as 2C (Fig 3B). This suggests that dMyc plays an important role in establishing proper gland growth and ploidy.

We hypothesized that the reduced ploidy and size of glands with reduced dMyc would affect proper gland function. To confirm this, we used a sperm competition assay. We crossed red-eyed males (either a red-eyed control or red-eyed male with AGs depleted for dMyc) with white-eyed females that were pre-mated to white-eyed males. We used eye color to track the percentage of F1 progeny that arise from the pre-mating versus the second mating to animals with reduced dMyc. In our control samples, we report a range from 15-30% of F1 progeny with red eyes, resulting from the second mating with a red-eye control male for crosses that contain 2-5 males each. From males with reduced dMyc we observed fewer progeny from the second mating, suggesting these males have reduced fertility or reduced sperm competitiveness. By contrast, animals with reduced Yki exhibited no defects in sperm competition (Supplement 3B). This suggests that main cell endocycling is important for proper gland function.

Juvenile Hormone (JH) signaling has been shown to promote accessory gland growth and protein synthesis in Drosophila and other insects (Herndon et al., 1997; Shemshedini, Lanoue, & Wilson, 1990; R. Yamamoto, Bai, Dolezal, Amdam, & Tatar, 2013). To test whether JH signaling may play a role in main cell endocycling on the day of eclosion in *Drosophila* accessory glands, we expressed RNAis to the JH nuclear receptors, Gce (germ

cell-expressed bHLH-PAS) or Met (Methoprene tolerant), or their co-activator Tai (Taiman). We find that RNAi to Gce and the co-activator Tai abolish EdU incorporation in the AG on the day of eclosion (Fig 3C). For both manipulations this resulted in reduced ploidy at day 10 (Fig 3B), with a total loss of the 8C population observed in controls, suggesting that JH signaling through Gce is necessary for proper main cell endocycles. Consistent with the reduced ploidy, we also see a decrease in overall size of the adult gland when JH signaling is inhibited (Fig 3D), suggesting early gland growth is driven in part by endocycles. Reduced gland growth also correlated with reduced fertility (Fig 3E), suggesting that the developmental endocycle that occurs shortly post eclosion is critical to proper gland maturation and function.

Main cells of the adult accessory gland remain poised to endocycle

We show that only a subset of main cells in the adult accessory gland continue to endocycle throughout the fly's lifespan (Fig 1). We therefore wondered if most main cells are robustly quiescent or if they remain in a poised state, ready to endocycle in response to cell cycle or cell growth signals.

We used the FLP-FRT system to create clones that express cell cycle and growth regulators in the adult gland (Fig 4A). In brief, this method uses a *hs-flp* to recombine FRT sites in an actin promoter-driven "flipout cassette" (act-FRT-stop-FRT-Gal4). Upon removal of the stop codon, the actin promoter leads to constitutive expression of Gal4 and permanent induction of UAS transgenes. Using this method we titrated the heat-shocks to control the number of cells that express Gal4 and induce subsets of cells in the adult gland to overexpress E2F1/DP with other known endocycle growth regulators that could increase the amount of main cell endocycling. We induced ectopic expression of E2F1/DP with dMyc in a subset of adult main cells 24h post eclosion. This misregulated expression led to dramatic increases in nuclear size and DNA content, easily observable by DAPI staining in adult main cells (Fig 4A).

The ease with which subsets of cells were able to enter additional, ectopic endocycles led us to ask if the overall gland has this same plasticity. We used Prd-Gal4 to drive overexpression or RNAi of common endocycle regulators to address this question.

We find that driving expression of E2F/DP, Rbf RNAi, and CyclinD/CDK4 all resulted in glands with enlarged main cell nuclei (Fig 4B).

We confirmed that enlarged nuclei were due to the presence of ectopic S-phases in the adult tissue using a one-day EdU/sucrose feeding on animals at 14 days post eclosion when expressing E2F1/DP with dMyc, Yki or constitutively active Yki (Yki*) (Fig 4C). This results in an extensive increase in both nuclear area and variation of nuclear size (Fig 4D). The ease with which the main cells of the accessory gland can be pushed to endocycle suggests that the adult gland retains more plasticity than previous thought.

The adult accessory gland can recover from damage

Due to the importance of the accessory gland for successful reproduction, we postulated that this tissue remains poised to endocycle in order to respond to cell loss or damage. To test this, we used the DEMISE system to induce cell death in the gland. The DEMISE system uses a heat-shock-flippase (*hs-Flp*) with a UAS-driven "flipout cassette" to induce controlled Reaper expression, driving caspase dependent apoptosis (Cohen, Allen, Sawyer, & Fox, 2018). We find that the DEMISE system effectively induces apoptosis in the AG (Fig 5). While the DEMISE system contains a *hs-Flp* to induce damage temporally, we quickly realized that a background level of damage already occurred in a heat shock-independent manner in the late pupal AG (after 60h APF) when reared at room temperature. We used this "leaky" *hs-Flp*-independent induction of damage to our advantage. When we dissect accessory glands expressing DEMISE on the day of eclosion, we find that 100% of glands show damage in at least one lobe with the majority of samples exhibiting one lobe with more extreme damage than the other (Fig 5B, Fig 5E). Using DCP1 staining, we verified higher levels of DCP1 staining occurs in the lobe that exhibits more damage and more pyknotic nuclei (Supplement 4). Importantly, the pyknotic nuclei were binucleate, indicating that DEMISE induces apoptosis in accessory gland cells after the binucleation event during development (Supplement 4).

We established a recovery protocol, in which we collected animals the day of eclosion, when 100% of animals we tested exhibit damage, and immediately shifted them to 18°C for 5 days to reduce the Gal4/UAS-driven Reaper expression and allow for some level of recovery. Using this protocol, we observed a striking recovery of gland morphology

and size (Fig 5C). After 5 days of recovery only 20% of animals show obvious defects in both gland lobes, compared to 100% of animals that show damage to at least one lobe on the day of eclosion (Fig 5D,E). In contrast, if animals expressing DEMISE are not shifted to 18°C and instead are left at room temperature, 90% of animals exhibit tissue damage (Supplement 4).

Compensatory cellular hypertrophy contributes to accessory gland tissue recovery from damage

Upon injury, tissues that have a mitotic population increase cell division to allow for regeneration after damage; however, we do not observe an obvious mitotic population in the adult AG. One mechanism of tissue repair in post-mitotic tissues is compensatory cellular hypertrophy (CCH), an increase in cell size that stems from increased endoreplication (Tamori & Deng, 2013). Similarly, diploid post-mitotic tissues can exhibit wound induced polyploidization (WIP), which can be a result of cell fusion, but is also driven in part by endocycling (Grendler, Lowgren, Mills, & Losick, 2019; Losick, Fox, & Spradling, 2013; Losick, Jun, & Spradling, 2016). Because the adult AG maintains the capacity to endocycle, we examined whether this tissue may exhibit features of CCH and/or WIP during gland recovery.

Because leaky induction of damage often occurs at a higher level in one accessory gland lobe rather than equally in both, it created an opportunity to compare gland recovery in lobes with high levels of damage vs. lower levels. After recovery from damage, lobes with more pyknotic nuclei exhibit a greater variation in cell and nuclear size, consistent with CCH (Fig 5F,G). We never observed gland cells with more than two nuclei under any damage or recovery protocol, suggesting the cell fusion aspect of WIP is absent in this tissue.

We next tested whether recovery from damage leads to an increase in endocycling. We used DEMISE induced damage followed by a longer recovery while using our EdU-feeding protocol to label cells that endocycle during recovery. Animals were raised at room temperature, collected the day of eclosion, and shifted to 18°C for 11 days and fed EdU/sucrose for the entire recovery. We observed increased levels of EdU incorporation in animals undergoing recovery as compared to control animals (Fig 6A, Fig 6B full recovery).

To address whether there is a critical time window for damage induced endocycling, we performed the same recovery protocol, except that animals were reared on standard CM for the first 5 days and fed EdU/sucrose for only the remaining 6 days. Again, we observed increased endocycling throughout the gland even after 5 days of recovery, demonstrating that the increased endocycling is not limited to an early acute damage response (Fig 6B, late recovery). DNA content measurements taken post recovery show populations of nuclei that are 16C and even up to 32C, with the EdU positive population showing increased DNA content compared to the EdU negative population (Fig 6C). This suggests that main cells of the adult AG remain poised to endocycle in response to tissue damage, in a manner similar to CCH.

We next asked whether gland recovery from damage could restore gland function and male fertility. To monitor the fertility of the animals, we used mating assays in which we mated individual males with virgin females and counted the total number of offspring. When DEMISE is active at 25°C, accessory gland size and number of offspring are significantly reduced (Fig 6D, Fig 6F). After 5 days of recovery at 18°C, gland size is partially restored and there is no significant difference in the number of offspring from the damaged flies compared to 18°C control animals (Fig 6E, Fig 6F). Importantly, the recovery protocol allows for restoration of tissue size even without mating (Fig 5-virgins, Fig 6-mated), indicating that the adult gland can recover from damage regardless of mating status. Altogether our data suggests the accessory gland can recover after damage in a manner that restores tissue mass and function, at least in part through compensatory cellular hypertrophy. We propose this is a novel model for postmitotic regeneration in an adult tissue.

Discussion

Here we describe contexts for endocycling in the main cells of the accessory gland (AG). We elucidate a role for juvenile hormone signaling in an adult-stage developmental endocycle and establish methods to block or promote accessory gland endocycles. Finally, we show that the main cells of the adult AG remain poised to endocycle, possibly to maintain proper tissue function throughout the lifespan and to allow for tissue regeneration upon damage. Our work establishes that main cells of the adult AG are not quiescent, but instead exhibit

low levels of endocycling normally and remain poised to endocycle in response to specific signals in order to maintain AG function.

Endocycling in accessory gland maturation and tissue homeostasis

We describe a previously unappreciated wave of endocycling that occurs in most, if not all, main cells of the AG shortly post-eclosion. Our data implies that this wave of endocycling and the resulting early gland growth is important for gland maturation and function.

We report that similar to other endocycling tissues, APC/C activity oscillations are required for proper endocycling. Additionally we show that the E2F/Rb network is critical for the endocycling status of the adult AG main cells, however our results suggest that this might occur in non-canonical fashion in which E2F2, which normally serves as a repressor of cell cycle genes, is necessary together with E2F1 function for induction of the developmental endocycle on the day of eclosion. There may be a tissue-specific non-repressor role for E2F2 in the AG, as tissue-specific knockdown of E2F2 by RNAi phenocopied the loss of gland endocycling in an *e2f2* null mutant background. Further studies will be needed to parse the functions of the E2F complexes in this tissue.

Juvenile hormone has previously been shown to promote AG growth (Herndon et al., 1997; Shemshedini et al., 1990; T. G. Wilson, DeMoor, & Lei, 2003; K. Yamamoto, Chadarevian, & Pellegrini, 1988). Here we show that endoreplication, gland size, and overall fertility are affected when this signaling pathway is disrupted. This opens an intriguing new field of study on what downstream factors juvenile hormone is regulating to induce the developmental endocycle shortly post-eclosion. Juvenile hormone signaling is already known to promote fat body polyploidization in females for vitellogenesis, through regulation of several cell cycle factors including DNA replication and licensing factors (Wu et al., 2018, Wu et al., 2020). Our work reveals a potentially parallel function for juvenile hormone signaling to promote fertility in males which may directly or indirectly regulate dMyc and the RB/E2F network in the accessory gland.

Main cells of the accessory gland remain poised to endocycle throughout the fly's lifespan. We find upregulation of factors previously implicated in growth-dependent endocycling mechanisms, E2F1/DP, dMyc, Yki and Yki* are sufficient to induce increased levels of endocycling. This shows that the gland is not robustly quiescent as previously

thought, but instead the adult tissue maintains plasticity to respond to cues, potentially both internally and externally. This may be advantageous to allow males to recover from temporary reproductive dormancy, which can be induced by environmental factors (Kubrak et al., 2016). It will be interesting to investigate whether endocycling in the AG plays a role in recovery of male fertility after reproductive dormancy.

The adult accessory gland as model for tissue regeneration

Our work reveals that the adult accessory gland retains the capacity to undergo growth and regeneration upon tissue damage. This tissue exhibits hallmarks of compensatory cellular hypertrophy (CCH) during recovery from damage, including increased cell and nuclear size along with increased EdU labeling and increased ploidy. These results are the first to establish the *Drosophila* accessory gland as a model for studying mechanisms that drive tissue regeneration in a non-mitotic, polyploid tissue. Since our assays for endocycling, and cell/nuclear ploidy involve tissue dissection and fixation, we established a line expressing RFP in the accessory gland along with DEMISE (Supplement 4). Using this line, we are able to track gland fluorescence to potentially monitor tissue loss and recovery within the same animal. We see a loss of fluorescence in animals undergoing active DEMISE, and an increase of gland fluorescence in animals that have undergone a recovery protocol. These results suggest that this paradigm can be used in high-throughput screens to determine genetic factors that influence post-mitotic regeneration via a non-dissection based method.

With tissue recovery after damage we also see functional restoration of the accessory gland. This is exciting as it establishes that the accessory gland can be used as a model to study regeneration in the context of fertility. The mammalian prostate also shows regenerative capacity upon partial prostatectomy (Isaacs, 2008), however many treatments for prostatic diseases can result in male infertility. It is important to establish additional working models to study infertility in the context of regeneration. Overall, our work establishes the *Drosophila* accessory gland as an excellent model for studying prostate regeneration and fertility restoration after large scale tissue damage.

Methods

Fly stocks

Canton-S (BL#64349)
w^{1118} (isogenic, BL#6326)
Prd-Gal4 (BL#1947) w[*]; Prd-Gal4/TM3, Sb[1]
Rbf RNAi: W; if/cyo (lacz); UAS-Rbf RNAi VDRC GD4484
Rbf280 (BL#50748): w[*]; P{w[+mC]=UAS-Rbf.280}3/TM3, Sb[1]
Dk4: y,w,hs-flp; UAS CycD, UAS-Cdk4/ CyO-GFP; Sb/TM6B
E2f1 RNAi: (BL# 27564) y,v; UAS-E2F1 RNAi JF02718
E2f2 RNAi (BL#36674): y[1] sc[*] v[1] sev[21]; P{y[+t7.7] v[+t1.8]=TRiP.HMS01562}attP2
Rca1: y,w, hs-flp; Pin/CyO-GFP; UAS-HA-Rca1/TM6B (Buttitta et al., 2010)
Ek2: y,w, hs-flp; +; UAS-CycE,UAS-Cdk2/TM6B (Buttitta et al., 2007)
Gce RNAi (BL#26323): y[1] v[1]; P{y[+t7.7] v[+t1.8]=TRiP.JF02097}attP2
Tai RNAi (BL#32885): y[1] sc[*] v[1] sev[21]; P{y[+t7.7] v[+t1.8]=TRiP.HMS00673}attP2
Met RNAi (BL#26205): y[1] v[1]; P{y[+t7.7] v[+t1.8]=TRiP.JF02103}attP2
dMyc RNAis (BL#25783): y[1] v[1]; P{y[+t7.7] v[+t1.8]=TRiP.JF01761}attP2, (BL#25784): y[1] v[1]; P{y[+t7.7] v[+t1.8]=TRiP.JF01762}attP2, (BL#51454): y[1] v[1]; P{y[+t7.7] v[+t1.8]=TRiP.HMC03189}attP40
y,w,hs-flp^{12}; UAS-E2F, UAS-DP/Cyo-GFP; UAS-$dMyc^{42}$/TM6B (UAS E2F1,UAS DP from Neufeld et al 1998, dMyc from BL#9675)
y,w,hs-flp^{12}; UAS-E2F, UAS-DP/Cyo-GFP; yki : (UAS E2F1,UAS DP from Neufeld et al 1998, yki from BL#28819)
y,w,hs-flp^{12}; UAS-E2F, UAS-DP/Cyo-GFP; yki* : (UAS E2F1,UAS DP from Neufeld et al 1998, Constitutively active UAS-Yki* from BL#28817)
w; UAS-P35/Cyo-GFP; act>CD2>gal4,UAS-GFP(nls)/TM3-Ser-GFP (UAS-P35 BL#5072, act>CD2>Gal4 from BL#4780)
DEMISE lines: 5-1, 9-1, 10-1, 10-2, 10-3 :: pUAST-FRT-Stop-FRT-rpr/CyO (provided by D. Fox)
y,w,hs-flp; +; Prd-gal 4/TM6B (y,w,hs-flp^{12} and BL#1947)
Fly FUCCI: (BL#55122) w[1118]; Kr[If-1]/CyO, P{ry[+t7.2]=en1}wg[en11]; P{w[+mC]=UAS-GFP.E2f1.1-230}26 P{w[+mC]=UAS-mRFP1.NLS.CycB.1-266}17/TM6B, Tb
RGB Cell Cycle Sensor: P{w{+mC}=UAS-nlsCdt1N101EBFP2-T2A-nlsCycBN96-nlsCycBN285tdTomato-T2A-EGFPPCNA} II.1 (UAS-RGB cell cycle tracker) (Handke et al., 2014)
EGFP::PCNA (provided by S. Blythe)
y,w,hs-flp;+; Prd-gal4, UAS-His2Av::RFP/TM6B
mCherry RNAi (BL#35785): [1] sc[*] v[1] sev[21]; P{y[+t7.7] v[+t1.8]=VALIUM20-mCherry}attP2
w; UAS-P35/Cyo-GFP; act>CD2>gal4,UAS-GFP(nls)/TM3-Ser-GFP (UAS-P35 BL#5072, act>CD2>Gal4 from BL#4780)

Fly rearing and mating

All flies were raised and kept at room temperature (23°C) on Bloomington Cornmeal food unless otherwise noted. For experiments with virgins: males were collected as virgins and aged for

indicated times in vials containing 7-10 males. For experiments with mated animals: males and females were kept at an approximate 1:1.5 ratio for indicated times unless otherwise stated.

Tissue fixation and staining

Accessory glands were dissected in 1X PBS and were fixed in 4% PFA+1xPBS for 30 min at room temperature while rocking. Tissues were rinsed with 1xPBS+0.1%Triton-X twice for 10 minutes. Tissues were further permeabilized in 1xPBS+1.0%Triton-X for 30 minutes at room temperature while rocking. Tissues were rinsed with PAT for 10 min and primary antibodies diluted in fresh PAT were incubated at room temperature rocking overnight. Tissues were rinsed twice for 10 minutes in 1xPBS+0.1%Triton-X. Tissues were pre-blocked in PBT-X+2%NGS for 10 minutes. Secondary antibody was added to fresh PBT-X+2%NGS and tissues were incubated overnight rotating at room temperature. Tissues were rinsed twice in 1xPBS+0.1%Triton-X before incubating in DAPI (1µg/ml) for 10 min. Tissues were rinsed thoroughly before mounting with Vectashield.

The following antibodies were used in this study: Mouse anti DLG (DHSB) 1:500, Rabbit anti PH3 (Millipore #06-570) 1:1000, mouse anti PH3 (Cell Signaling #9706) 1:1000, Rabbit anti DCP1 (Cell Signaling) 1:500.

EdU labeling

Click-IT EdU AlexaFluor-555/488 Imaging kits were used as directed (Life Technologies).

For labeling on the day of eclosion, accessory glands were dissected within 3 hours post-eclosion and immediately placed in Ringers solution containing 1mM EdU for 1 hour prior to fixing.

For longer term adult labeling, animals were fed 1 mM EdU in 10% sucrose with blue food coloring for the indicated amounts of time. EdU/sucrose mixture was placed on whatman paper within empty vials and was changed every 2-3 days to control for contamination. We also performed feeding with 1 mM EdU in Cornmeal food with blue food coloring for up to 6 days and obtained similar results.

Measurements/DAPI quantifications

Fluorescent images were obtained using a Leica SP5 confocal, Leica SP8 confocal or Leica DMI6000B epifluorescence system. Brightfield images used to quantify gland size were taken on a Leitz Orthoplan.

To obtain overall gland size measurements, images were imported to Adobe Photoshop and Lasso Tool was used to outline the lobe of the accessory gland. Photoshop Measure was used to quantify pixels within the gland and measurements were transferred to Prism for analysis.

Discs large (DLG) antibody staining was used for all cell size measurements. Due to the apical localization of DLG, cell size measurements reported here are not of the volume of a cell, but rather a measurement of the apical area. Measurements reported here are taken mid-lobe and

are only of main cells to ensure cell type differences are not confounding our measurements. Image J was used to obtain measurements of cells in microns and measurements were transferred to Prism for analysis.

Nuclear area measurements were done similarly to cell size (described above) using DAPI signal to delineate nuclei and include main cells only.

To obtain ploidy measurements, we modified a protocol from the Losick Lab (Grendler et al., 2019) for this tissue. In brief: DAPI was carefully imaged using Leica SP5 confocal system and intensity quantifications were measured using ImageJ. Raw Integrated Intensity measurements were used for the binucleated cells from the mid-lobe region of the accessory gland and the mononucleated, basally located, diploid muscle nuclei of the ejaculatory duct where Paired-gal4 is not expressed. The average background fluorescence was subtracted from each intensity measurement to get the corrected intensity. Intensity for haploid DNA content was deduced by dividing the average intensity of the ejaculatory duct nuclei in half. Ploidy of the accessory gland nuclei was established using the following binning: 2N (1.9-2.9), 4N (3.0-6.9), 8N (7-12.9), 16N (13.0-24.9), 32N (>24.9).

Fertility

Fertility assays (Fig 3E): We modified a previously established method from the Bach Lab (Herrera et al., 2021). In brief: virgin males of stated genotypes and Canton S virgin females were collected between 16-24 hours prior to starting assay. 2 Canton S virgins and 1 virgin male of stated genotype were mated for two days at 25°C. Total offspring arising from the individual crosses were counted.

DEMISE fertility assays (Fig 6F): Individual virgin males were collected on the day of eclosion and were crossed with 15 Canton S virgin females (0-3 days of age).
For DEMISE active assay: Virgin males were collected on the day of eclosion, crossed with virgin females, and kept at 25°C for the duration of the experiment.
DEMISE recovery fertlity assay: Virgin males were placed at 18°C for 5 day recovery period prior to mating and the flies were kept at 18 for the duration of the mating. For all experiments: Vials in which animals had laid in and were flipped out of were placed at 25°C to allow for proper development. Crosses were flipped every 2-3 days. Total number of progeny was counted.

Sperm competition assay (Supplement 3): Groups of 3-5 males were mated with w^{1118} females pre-mated with w^{1118}. Males were placed with females within 24 hours of eclosion. Females were 1-5 days of age from bottles, all having mated previously (no virgin females were collected for this assay). Animals were left to mate for a total of 7 days and were flipped into new vials every 2-3 days. The percentages reported are the total number of red-eyed offspring that emerge from each vial. All mating and development was done at 25C.

Statistical Analysis

All statistics were run using Prism Graphpad using ordinary one-way anova.

DEMISE

When kept at room temperature, on the day of eclosion animals already show DEMISE induced damage. For recovery experiments animals were collected as virgins and shifted to 18°C to reduce the Gal4/UAS expression levels. For EdU experiments animals were fed EdU/sucrose as described above for the indicated amounts of time.

Induction of growth regulators

For EdU labeling: Newly eclosed flies were heat-shocked at 37°C for 20 min and aged for 14 days. Flies were fed EdU/sucrose as described above for 24 hours prior to dissection.

Acknowledgements:

We thank members of the Buttitta and Taichman Labs for advice and discussions, especially Ajai Pulianmackal, Dr. Frank Cackowski and Dr. Kenji Yumoto. We thank Pusparanee Hakim, David Hayes and Ce Wang for help with early experiments characterizing the fly AG and Yukiko Yamashita for helpful discussion. We thank the following for kindly providing fly lines: Shelby Blythe for PCNA::GFP, Erez Cohen and Don Fox for DEMISE lines, and Christian Lehner for the RGB line. This work was supported by a Prostate Cancer Foundation Challenge Award (16CHAL05) and an American Cancer Society Scholar Award (RSG-15-161-01-DDC). A. Box was supported by the University of Michigan Organogenesis Predoctoral Training Grant (NIH T32 HD007505) and an NRSA Predoctoral Fellowship (NIH F31 HD103430-01). S.J. Church was supported by a University of Michigan Rackham Merit Fellowship and S. Nandakumar was supported by a University of Michigan Barbour Scholarship. Work in the Buttitta Lab is also supported by the National Institute of General Medical Sciences (NIH R01 GM127367).

Adams, E. M., & Wolfner, M. F. (2007). Seminal proteins but not sperm induce morphological changes in the Drosophila melanogaster female reproductive tract during sperm storage. *Journal of Insect Physiology*, *53*(4), 319–331. https://doi.org/10.1016/j.jinsphys.2006.12.003

Ahmad, S. M., & Baker, B. S. (2002). Sex-Specific Deployment of FGF Signaling in Drosophila Recruits Mesodermal Cells into the Male Genital Imaginal Disc. *Cell*, *109*, 651–661. Retrieved from https://ac.els-cdn.com/S0092867402007444/1-s2.0-S0092867402007444-main.pdf?_tid=1ad7399d-b7b3-468a-8533-ca50aaf0bfd7&acdnat=1542724232_d7718ef80de0595af0c37dbdfa969c9d

Bairati, A. (1968). STRUCTURE AND ULTRASTRUCTURE OF THE MALE REPRODUCTIVE SYSTEM IN DROSOPHILA MELANOGASTER MEIG. *Italian Journal of Zoology*, 105–182.

Bertram, M. J., Akerkar, G. A., Ard, R. L., Gonzalez, C., & Wolfner, M. F. (1992). Cell type-specific gene expression in the Drosophila melanogaster male accessory gland. *Mechanisms of Development*, *38*(1), 33–40. https://doi.org/10.1016/0925-4773(92)90036-J

Blythe, S. A., & Wieschaus, E. F. (2016). Establishment and maintenance of heritable chromatin structure during earlyDrosophilaembryogenesis. *ELife*, *5*. https://doi.org/10.7554/eLife.20148

Bosco, G., Du, W., & Orr-Weaver, T. L. (2001). DNA replication control through interaction of E2F–RB and the origin recognition complex. *Nature Cell Biology 2001 3:3*, *3*(3), 289–295. https://doi.org/10.1038/35060086

Cohen, E., Allen, S. R., Sawyer, J. K., & Fox, D. T. (2018). Fizzy-Related dictates A cell cycle switch during organ repair and tissue growth responses in the Drosophila hindgut. *ELife*, *7*. https://doi.org/10.7554/eLife.38327

Edgar, B. A., Zielke, N., & Gutierrez, C. (2014). Endocycles: a recurrent evolutionary innovation for post-mitotic cell growth. *Nature Reviews Molecular Cell Biology*, *15*(3), 197–210. https://doi.org/10.1038/nrm3756

Flegel, K., Grushko, O., Bolin, K., Griggs, E., & Buttitta, L. (2016). Roles for the Histone Modifying and Exchange Complex NuA4 in Cell Cycle Progression in Drosophila melanogaster. https://doi.org/10.1534/genetics.116.188581

Grendler, J., Lowgren, S., Mills, M., & Losick, V. P. (2019). Wound-induced polyploidization is driven by Myc and supports tissue repair in the presence of DNA damage. *Development (Cambridge, England)*, *146*(15). https://doi.org/10.1242/DEV.173005

Handke, B., Szabad, J., Lidsky, P. V., Hafen, E., & Lehner, C. F. (2014). Towards Long Term Cultivation of Drosophila Wing Imaginal Discs In Vitro. *PLoS ONE*, *9*(9), e107333. https://doi.org/10.1371/journal.pone.0107333

Heifetz, Y., Vandenberg, L. N., Cohn, H. I., & Wolfner, M. F. (2005). Two cleavage products of the Drosophila accessory gland protein ovulin can independently induce ovulation. *Proceedings of the National Academy of Sciences*, *102*(3), 743–748. https://doi.org/10.1073/pnas.0407692102

Herndon, L. A., Chapman, T., Kalb, J. M., Lewin, S., Partridge, L., & Wolfner, M. F. (1997). Mating and hormonal triggers regulate accessory gland gene expression in male Drosophila. *Journal of Insect Physiology*, *43*(12), 1117–1123. https://doi.org/10.1016/S0022-1910(97)00062-0

Herrera, S. C., Sainz de la Maza, D., Grmai, L., Margolis, S., Plessel, R., Burel, M., … Bach, E. A. (2021). Proliferative stem cells maintain quiescence of their niche by secreting the Activin inhibitor Follistatin. *Developmental Cell*, *56*(16), 2284-2294.e6. https://doi.org/10.1016/J.DEVCEL.2021.07.010

Inge Øvrebø, J., & Edgar, B. A. (2018). Polyploidy in tissue homeostasis and regeneration. https://doi.org/10.1242/dev.156034

Leiblich, A., Hellberg, J. E. E. U., Sekar, A., Gandy, C., Mendes, C. C., Redhai, S., … Wilson, C. (2019). Mating induces switch from hormone-dependent to hormone-independent steroid receptor–mediated growth in Drosophila secondary cells. *PLOS Biology*, *17*(10), e3000145. https://doi.org/10.1371/journal.pbio.3000145

Leiblich, A., Marsden, L., Gandy, C., Corrigan, L., Jenkins, R., Hamdy, F., & Wilson, C. (2012). Bone morphogenetic protein- and mating-dependent secretory cell growth and migration in the Drosophila accessory gland. *Proceedings of the National Academy of Sciences of the United States of America*, *109*(47), 19292–19297. https://doi.org/10.1073/pnas.1214517109

Losick, V. P., Fox, D. T., & Spradling, A. C. (2013). Polyploidization and Cell Fusion Contribute to Wound Healing in the Adult Drosophila Epithelium. *Current Biology*, *23*(22), 2224–2232. https://doi.org/10.1016/J.CUB.2013.09.029

Losick, V. P., Jun, A. S., & Spradling, A. C. (2016). Wound-Induced Polyploidization: Regulation by Hippo and JNK Signaling and Conservation in Mammals. *PLOS ONE*, *11*(3), e0151251. https://doi.org/10.1371/journal.pone.0151251

Lung, O., Kuo, L., & Wolfner, M. F. (2001). Drosophila males transfer antibacterial proteins from their accessory gland and ejaculatory duct to their mates. *Journal of Insect Physiology*, *47*(6), 617–622. https://doi.org/10.1016/S0022-1910(00)00151-7

Maines, J. Z., Stevens, L. M., Tong, X., & Stein, D. (2004). Drosophila dMyc is required for ovary cell growth and endoreplication. *Development*, *131*(4), 775–786. https://doi.org/10.1242/dev.00932

Narbonne-Reveau, K., Senger, S., Pal, M., Herr, A., Richardson, H. E., Asano, M., … Lilly, M. A. (2008). APC/CFzr/Cdh1 promotes cell cycle progression during the Drosophila endocycle. *Development (Cambridge, England)*, *135*(8), 1451–1461. https://doi.org/10.1242/dev.016295

Orr-Weaver, T. L. (2015). When Bigger Is Better: The Role of Polyploidy in Organogenesis HHS Public Access. *Trends Genet*, *31*(6), 307–315. https://doi.org/10.1016/j.tig.2015.03.011

Pierce, S. B., Yost, C., Britton, J. S., Loo, L. W. M., Flynn, E. M., Edgar, B. A., & Eisenman, R. N. (2004). dMyc is required for larval growth and endoreplication in Drosophila. *Development*, *131*(10), 2317–2327. https://doi.org/10.1242/dev.01108

Prince, E., Kroeger, B., Gligorov, D., Wilson, C., Eaton, S., Karch, F., … Maeda, R. K. (2019). Rab-mediated trafficking in the secondary cells of *Drosophila* male accessory glands and its role in fecundity. *Traffic*, *20*(2), 137–151. https://doi.org/10.1111/tra.12622

Qazi, M. C. B., & Wolfner, M. F. (2003). An early role for the Drosophila melanogaster male seminalprotein Acp36DE in female sperm storage. *Journal of Experimental Biology*, *206*(19), 3521–3528. https://doi.org/10.1242/JEB.00585

Ravi Ram, K., Ji, S., & Wolfner, M. F. (2005). Fates and targets of male accessory gland proteins in mated female Drosophila melanogaster. *Insect Biochemistry and Molecular Biology*, *35*(9), 1059–1071. https://doi.org/10.1016/J.IBMB.2005.05.001

Shemshedini, L., Lanoue, M., & Wilson, T. G. (1990). Evidence for a juvenile hormone receptor involved in protein synthesis in Drosophila melanogaster. *Journal of Biological Chemistry*, *265*(4), 1913–1918. https://doi.org/10.1016/S0021-9258(19)39917-X

Sitnik, J. L., Gligorov, D., Maeda, R. K., Karch, F., & Wolfner, M. F. (2016). The Female Post-Mating Response Requires Genes Expressed in the Secondary Cells of the Male Accessory Gland in Drosophila melanogaster. *Genetics*, *202*(3), 1029–1041. https://doi.org/10.1534/genetics.115.181644

Susic-Jung, L., Hornbruch-Freitag, C., Kuckwa, J., Rexer, K.-H., Lammel, U., & Renkawitz-Pohl, R. (2012). Multinucleated smooth muscles and mononucleated as well as multinucleated striated muscles develop during establishment of the male reproductive organs of Drosophila melanogaster. *Developmental Biology*, *370*(1), 86–97. https://doi.org/10.1016/J.YDBIO.2012.07.022

Tamori, Y., & Deng, W.-M. (2013). Compensatory Cellular Hypertrophy: The Other Strategy for Tissue Homeostasis. https://doi.org/10.1016/j.tcb.2013.10.005

Taniguchi, K., Kokuryo, A., Imano, T., Minami, R., Nakagoshi, H., & Adachi-Yamada, T. (2014). Isoform-specific functions of Mud/NuMA mediate binucleation of Drosophila male accessory gland cells. *BMC Developmental Biology*, *14*, 46. https://doi.org/10.1186/s12861-014-0046-5

Von Stetina, J. R., Frawley, L. E., Unhavaithaya, Y., & Orr-Weaver, T. L. (2018). Variant cell cycles regulated by Notch signaling control cell size and ensure a functional blood-brain barrier. https://doi.org/10.1242/dev.157115

Wilson, C., Leiblich, A., Goberdhan, D. C. I., & Hamdy, F. (2017). The Drosophila Accessory Gland as a Model for Prostate Cancer and Other Pathologies. In *Current topics in developmental biology* (Vol. 121, pp. 339–375). https://doi.org/10.1016/bs.ctdb.2016.06.001

Wilson, T. G., DeMoor, S., & Lei, J. (2003). Juvenile hormone involvement in Drosophila melanogaster male reproduction as suggested by the Methoprene-tolerant27 mutant phenotype. *Insect Biochemistry and Molecular Biology*, *33*(12), 1167–1175. https://doi.org/10.1016/J.IBMB.2003.06.007

Xin, S., Weng, L., Xu, J., & Du, W. (2002). The role of RBF in developmentally regulated cell proliferation in the eye disc and in Cyclin D/Cdk4 induced cellular growth.

Yamamoto, K., Chadarevian, A., & Pellegrini, M. (1988). Juvenile hormone action mediated in male accessory glands of Drosophila by calcium and kinase C. *Science (New York, N.Y.)*, *239*(4842), 916–919. https://doi.org/10.1126/SCIENCE.3124270

Yamamoto, R., Bai, H., Dolezal, A. G., Amdam, G., & Tatar, M. (2013). Juvenile hormone regulation of Drosophila aging. *BMC Biology*, *11*, 85. https://doi.org/10.1186/1741-7007-11-85

Zielke, N., Querings, S., Rottig, C., Lehner, C., & Sprenger, F. (2008). The anaphase-promoting complex/cyclosome (APC/C) is required for rereplication control in endoreplication cycles. *Genes & Development*, *22*(12), 1690–1703. https://doi.org/10.1101/gad.469108

Zielke, Norman, Kim, K. J., Tran, V., Shibutani, S. T., Bravo, M. J., Nagarajan, S., … Edgar, B. A. (2011). Control of Drosophila endocycles by E2F and CRL4 CDT2. *Nature*, *480*(7375), 123–127. https://doi.org/10.1038/nature10579

Zielke, Norman, Korzelius, J., van Straaten, M., Bender, K., Schuhknecht, G. F. P., Dutta, D., … Edgar, B. A. (2014). Fly-FUCCI: A Versatile Tool for Studying Cell Proliferation in Complex Tissues. *Cell Reports*, *7*(2), 588–598. https://doi.org/10.1016/J.CELREP.2014.03.020

Zielke, Norman, Querings, S., Rottig, C., Lehner, C., & Sprenger, F. (2008). The anaphase-promoting complex/cyclosome (APC/C) is required for rereplication control in endoreplication cycles. https://doi.org/10.1101/gad.469108

Figures & Figure Legends
Fig.1

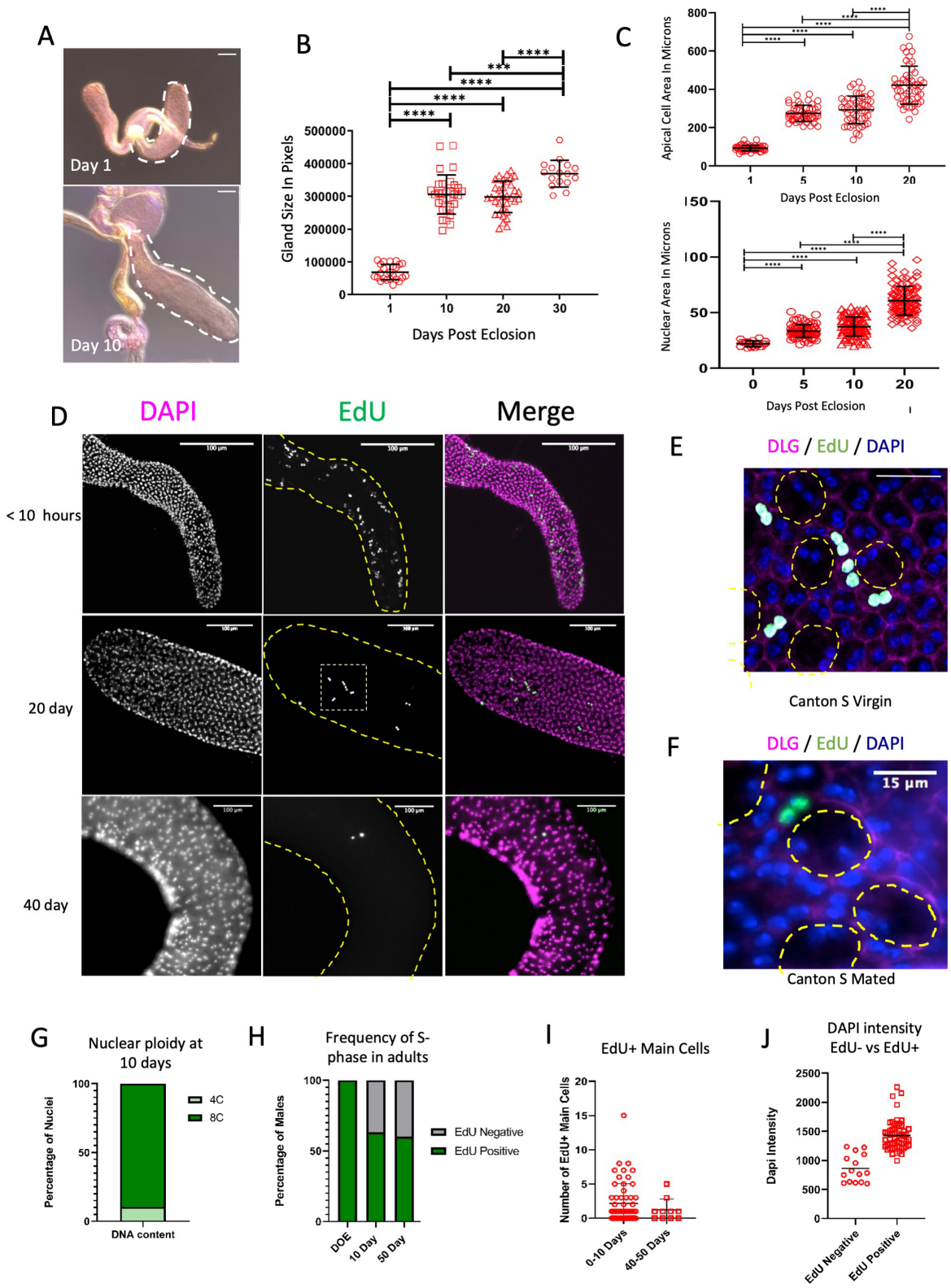

Figure 1: The adult accessory gland grows and main cells endoreplicate under normal physiological conditions throughout lifespan.

A: Adult accessory glands at day 1 (day of eclosion) and day 10 post eclosion. Accessory gland lobe is outlined with white dashed line. All glands measured are from virgins, so that size effects due to mating (i.e. release of seminal fluid proteins, hormonal signaling, muscle contractions, and emptying of the lumen) would not confound measurements.

B: Quantification of adult virgin male accessory gland area in pixels at indicated ages.

C: Quantification of adult virgin male accessory gland cell size and nuclear size in microns at indicated ages.

D: EdU incorporation assays in virgin male accessory glands. Accessory glands are outlined with yellow dashed line.

E: Magnified image from day 20 in panel D. EdU+ cells are main cells located near the distal tip of the gland. Secondary cells are outlined with yellow dashed line.

F: Representative magnified image from mated male accessory gland. EdU+ cell is a main cell near the distal tip of the gland. Secondary cells are outlined with yellow.

G: Quantification of nuclear DNA content represented as percentage of nuclei measured.

H: Frequency of entry into s-phase in the adult accessory gland represented as percentage of males EdU+ vs EdU-. DOE = day of eclosion.

I: Quantification of the number of EdU+ main cells per accessory gland during 10 day EdU feeding protocols.

J: Quantification of Dapi fluorescence intensity for EdU+ cells vs EdU- cells.

Statistics are one-way ANOVA:
**** $p < 0.0001$
*** $p = 0.0002$
Scale bars:
A,D: 100 microns
E: 25 microns
F: 15 microns

Fig 2

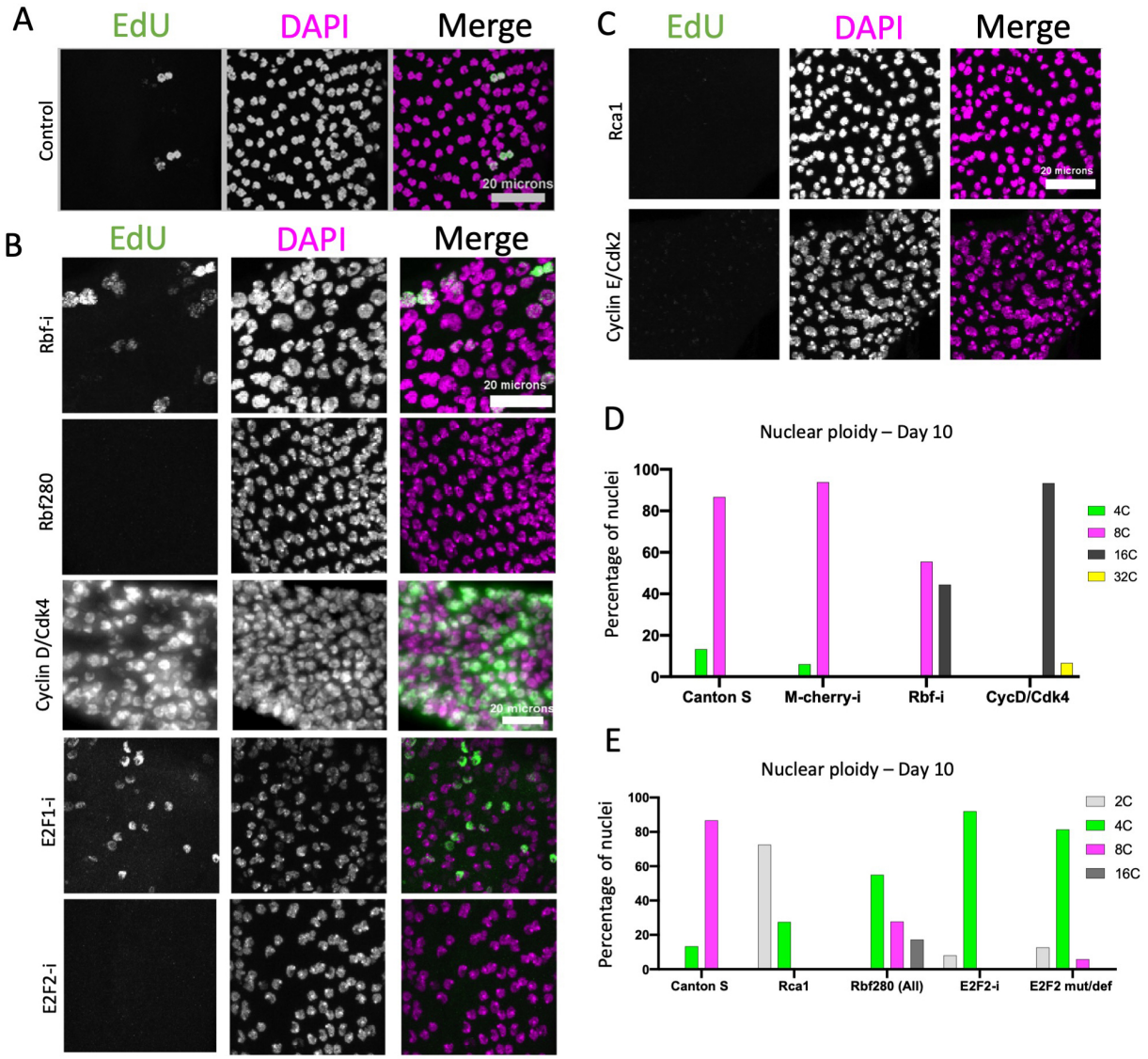

Figure 2: The E2F/RBf network and APC/C activity oscillations are required for developmental endocycle in the adult accessory gland

A-D: Representative images showing EdU incorporation in virgin male accessory glands on the day of eclosion.
A: Prd-Gal4 control
B: Prd-Gal4 driving expression of indicated transgenes to assay the role of the E2F/Rbf network in gland endocycling.
C: Prd-Gal4 driving expression of indicated transgenes to disrupt APC/C activity oscillations.

D: Quantification of nuclear DNA content for Day 10 virgins represented as percentage of nuclei measured. These are manipulations that increased ploidy.

E: Quantification of nuclear DNA content for Day 10 virgins represented as percentage of nuclei measured. These are manipulations that decreased ploidy.

Scale bars:
A,B,C: 20 microns

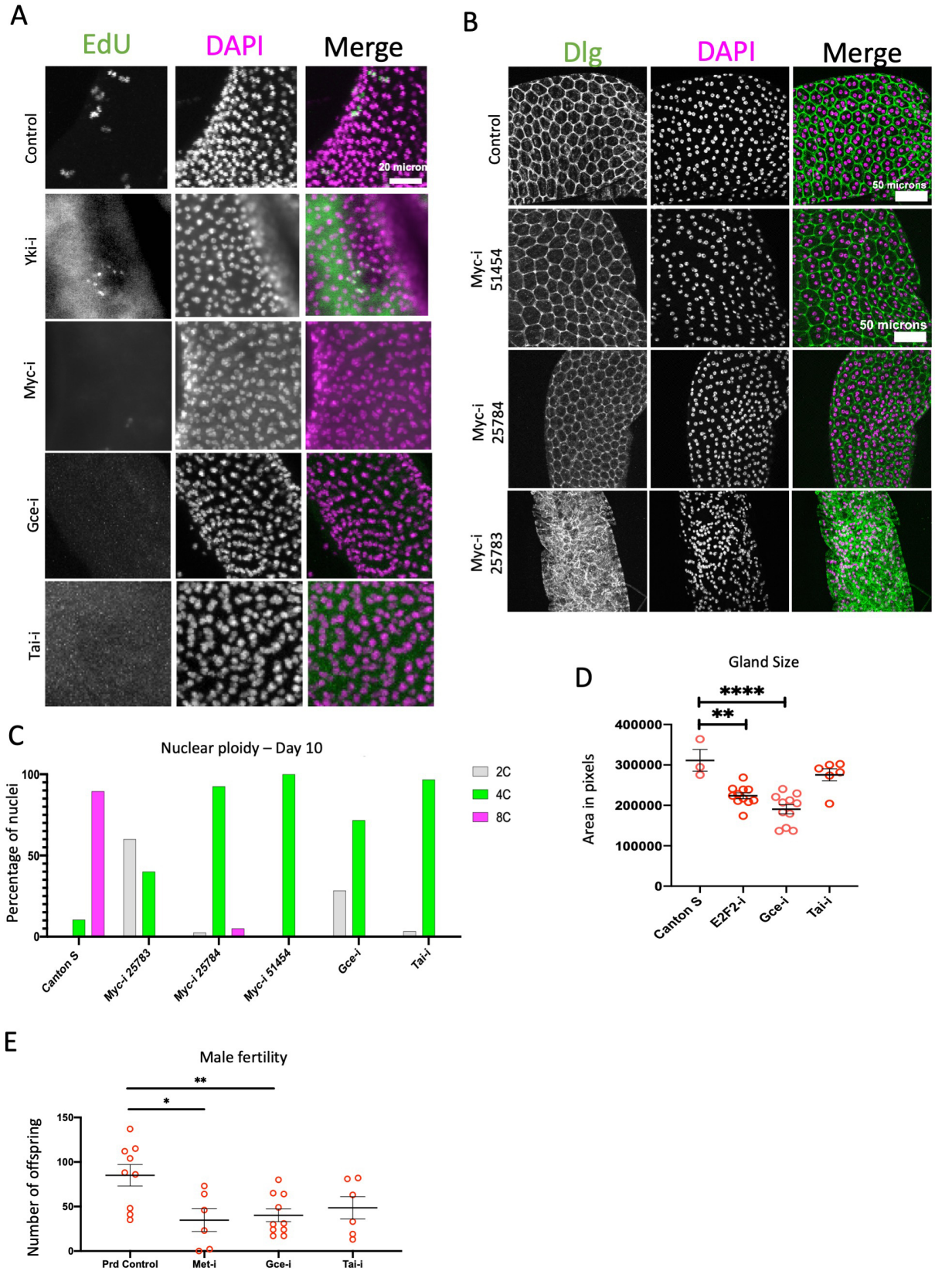
A
EdU
DAPI
Merge
Control
Yki-i
Myc-i
Gce-i
Tai-i
20 micron
B
Dlg
DAPI
Merge
Control
Myc-i 51454
Myc-i 25784
Myc-i 25783
50 microns
50 microns
C
Nuclear ploidy – Day 10
Percentage of nuclei
100
50
0
2C
4C
8C
Canton S
Myc-i 25783
Myc-i 25784
Myc-i 51454
Gce-i
Tai-i
D
Gland Size
****
**
Area in pixels
400000
300000
200000
100000
0
Canton S
E2F2-i
Gce-i
Tai-i
E
Male fertility
**
*
Number of offspring
150
100
50
0
Prd Control
Met-i
Gce-i
Tai-i

Figure 3: dMyc and Juvenile Hormone signaling are required for proper adult accessory gland endocycling and function

A: Representative images of EdU incorporation in virgin male accessory glands on the day of eclosion.

B: Adult accessory glands of 10 day virgin males. Prd-Gal4 expressing RNAi for dMyc. Loss of dMyc causes disruption of gland size, nuclear size, and overall gland morphology.

C: Quantification of nuclear DNA content at Day 10 represented as percentage of individual nuclei for indicated genotypes.

D: Total gland area measurements for 10 day adult accessory glands for indicated genotypes.

E: Results of fertility assays showing the total number of offspring that result from males of indicated genetic manipulations crossed to wild-type Canton-S females.

Statistics are one-way ANOVA
** $p=0.0012$
**** $p<0.0001$
Scale bars:
A: 20 microns
B: 50 microns

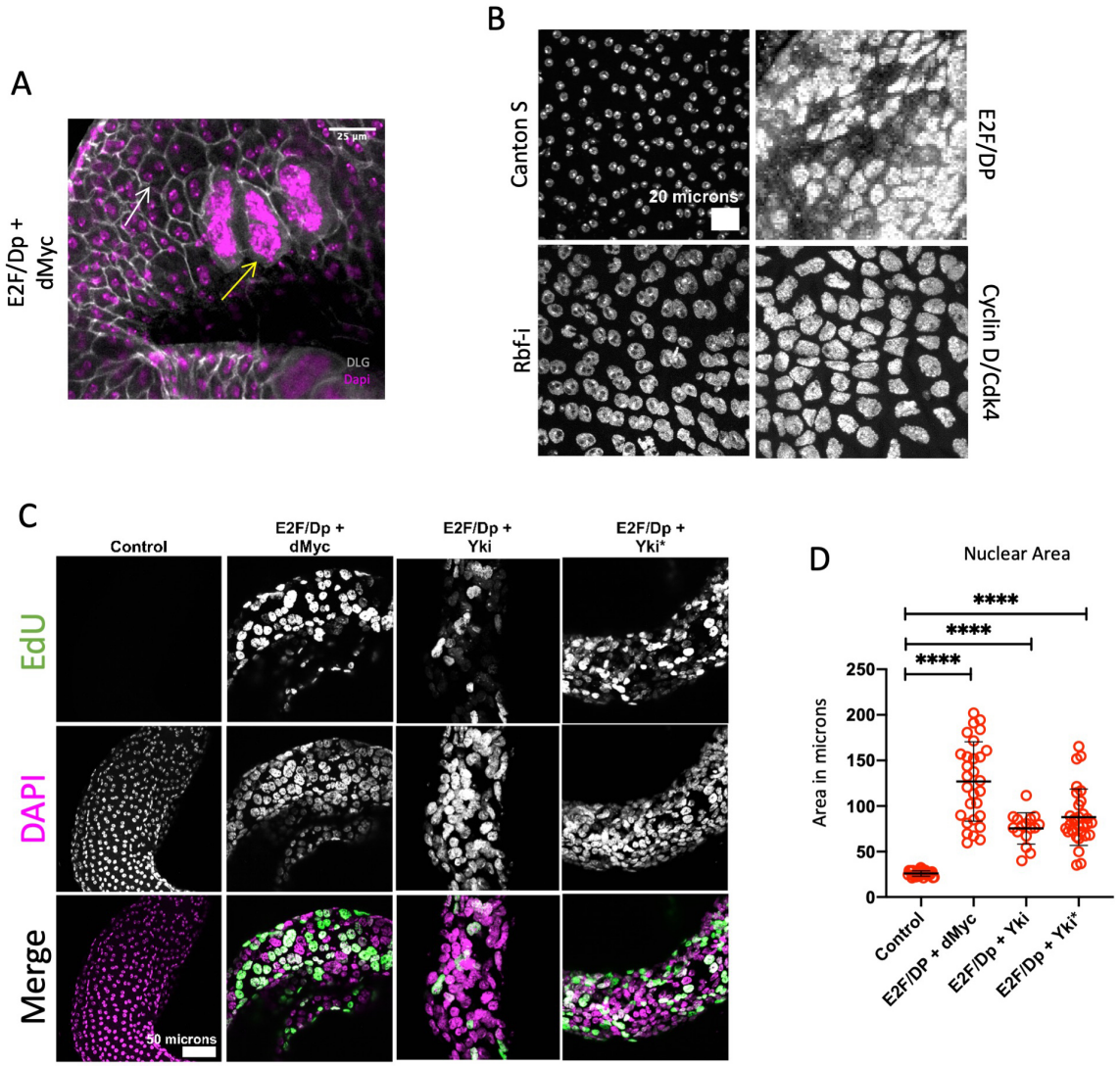

Figure 4: Main cells of the adult accessory gland remain poised to endocycle.

A: Clonal overexpression of E2F/DP with dMYC in the adult accessory gland. White arrows: normal nuclear morphology, Yellow arrows: enlarged nuclei.

B: Representative images of gland nuclei from Prd-Gal4 driving expression of indicated transgenes.

C: EdU incorporation with 1 day EdU feeding in the adult accessory gland upon overexpression of E2F/DP with indicated growth factor at 14 days post-eclosion/heatshock.

D: Nuclear area measurements of individual nuclei in adult accessory glands overexpressing E2F/DP with indicated growth factor at 14 days post-eclosion/heatshock.

Scale Bars:

A: 25 microns
B: 20 microns
C: 50 microns

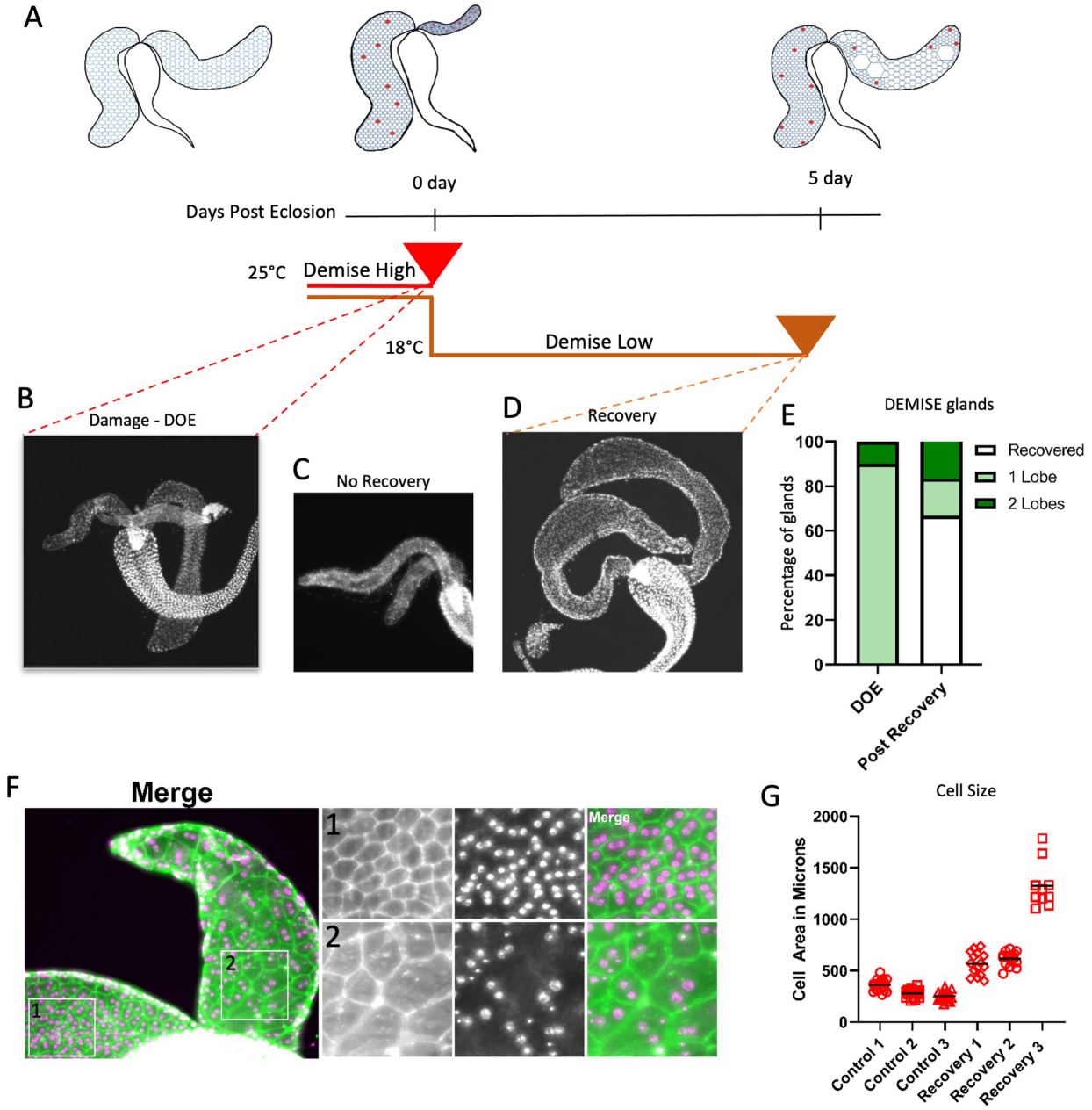

Figure 5: The adult accessory gland can recover from damage

A: Schematic of experimental procedure using DEMISE to induce damage and a recovery protocol in the accessory gland. Red cells represent cells with active DEMISE and high Reaper expression.

B: DEMISE induces damage in the adult accessory gland on the day of eclosion. One lobe exhibits higher levels of damage.

C: Adult accessory gland with DEMISE kept at room temperature for 3 days without recovery.

D: Adult accessory gland with DEMISE recovery protocol. This animal has been shifted to 18°C for 5 day recovery.

E: Quantification of DEMISE - induced damage on the day of eclosion and accessory gland phenotypes post-recovery via categories of: normal size lobes/fully recovered lobes, 1 damaged lobe, or 2 damaged lobes.

F: Accessory gland with DEMISE after damage recovery: one lobe (1) exhibits lower levels of hypertrophy while the other lobe (2) exhibits more compensatory cellular hypertrophy.

G: Cell area measurements of accessory glands that never had active DEMISE (control) and accessory glands that have undergone the recovery protocol (recovery).

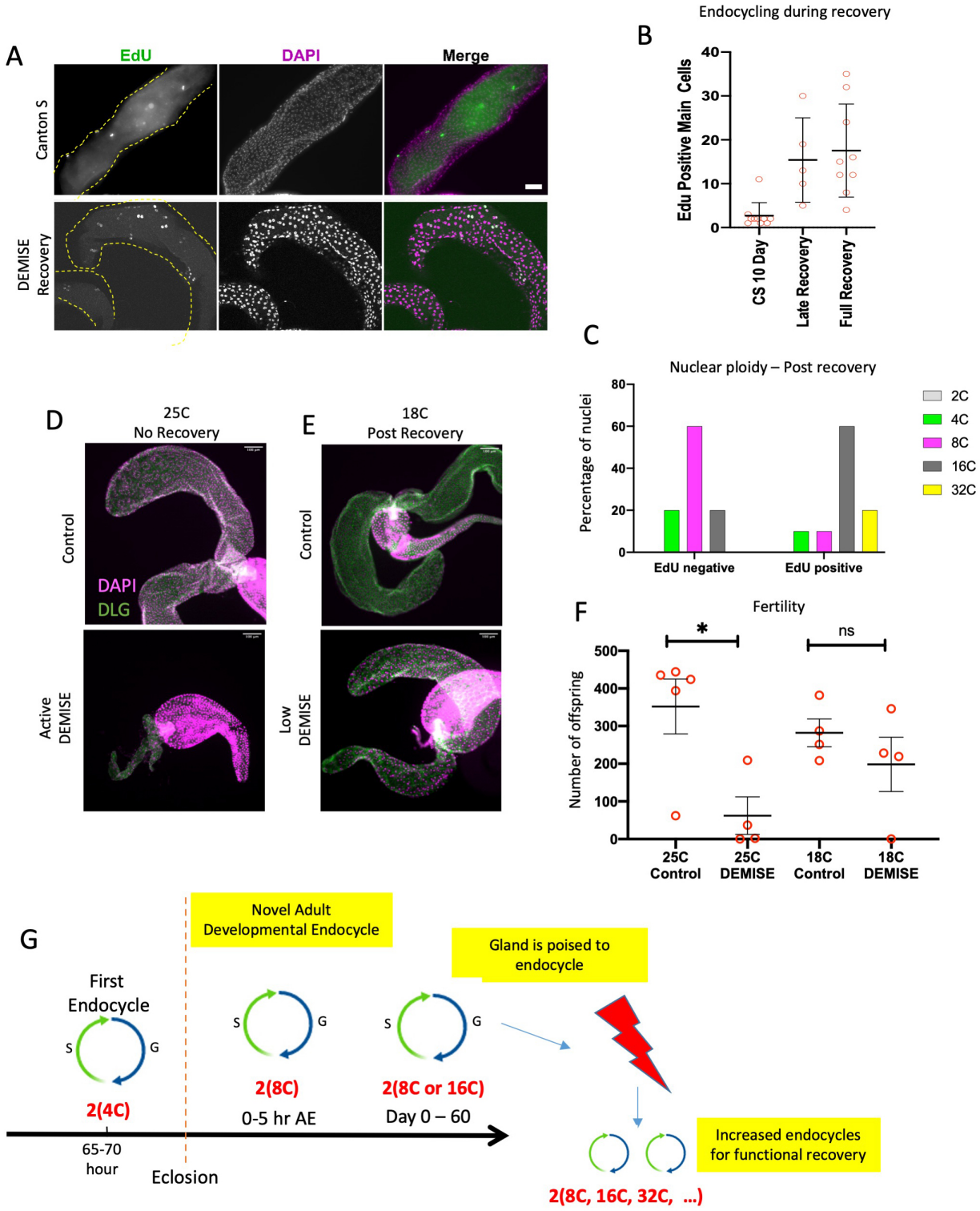

Figure 6: Adult accessory gland regeneration incorporates increased endoreplication and exhibits compensatory cellular hypertrophy

A: Representative images of accessory gland EdU incorporation in Canton S and DEMISE - damaged glands that have undergone recovery. 10 day EdU feeding occurs during recovery.

B: Quantification of EdU+ main cells. CS= 10 day Canton S control, Late recovery = EdU feeding only for the last 6 days of an 11day recovery timecourse. Full recovery = EdU feeding for the full 11 day recovery.

C: Quantification of nuclear DNA content of EdU- vs EdU+ nuclei. Males have had DEMISE – induced damage and were fed EdU during recovery.

D: Adult accessory glands of 10 day mated males kept at 25°C. Top panel – control with no active DEMISE, bottom panel – DEMISE active.

E: Adult accessory glands of 5 day mated males kept at 18°C. Top panel: control with no active DEMISE, bottom panel: DEMISE active, but underwent recovery at 18°C.

F: Total number of offspring for each mating condition: 25°C DEMISE active, 25°C DEMISE control, 18°C DEMISE recovery, and 18°C DEMISE recovery control. Controls are crosses containing DEMISE with no Gal4 driver.

G: Model: An additional endocycle occurs in main cells shortly post-eclosion. The mature gland exhibits rare endocycles and remains poised to endocycle in response to damage for functional recovery.

Statistics are one-way ANOVA
* $p = 0.0232$
Scale Bars
A: 50 microns
D,E: 100 microns

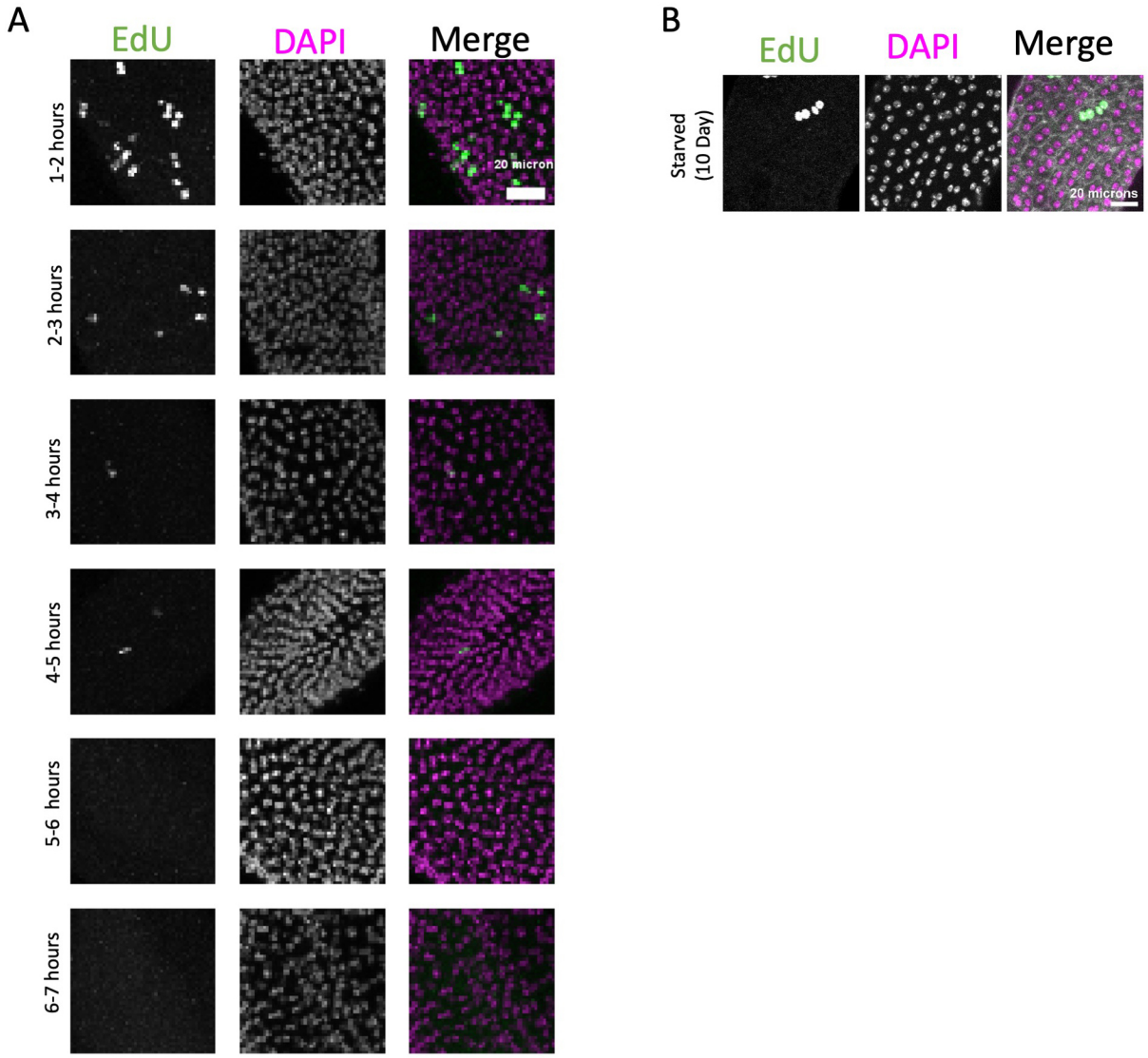

Supplemental Figure 1 : Endocycling in the adult accessory gland

A: Detailed timecourse of EdU incorporation between hours 1-7 post eclosion. Each timepoint was incubated with EdU for 1 hour post dissection, prior to fixation.

B: EdU incorporation occurs in starved animals (or animals fed sucrose water with EdU).

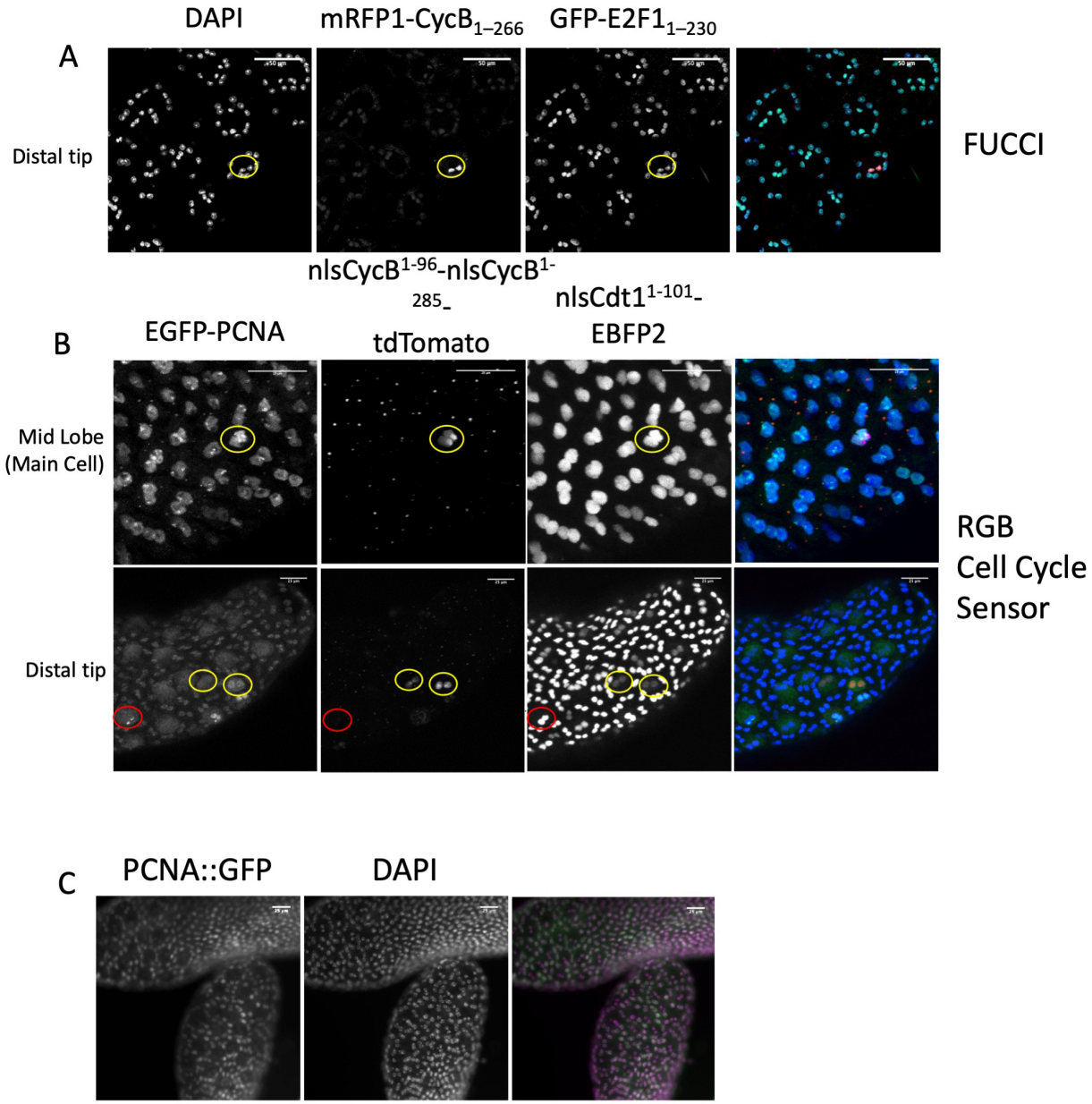

Supplemental Figure 2: Cell cycle degradation machinery oscillates in the adult accessory gland.

A: Prd-Gal4 driving fly FUCCI transgenes in the adult accessory gland. Cell cycle protein degrons mRFP1-CycB$_{1–266}$, to assay APC/C activity, and GFP-E2F1$_{1–230}$, to assay CRL4 (Cdt2) activity. The tissue has high APC/C activity, except in a small subset of cells, outlined in yellow.

B: Prd-Gal4 driving the RGB cell cycle sensor in the adult accessory gland. Full length EGFP-PCNA to visualize early S Phase and cell cycle protein degrons nlsCycB$^{1-96}$-nlsCycB$^{1-285}$-tdTomato, to assay APC/C activity, and nlsCdt1$^{1-101}$-EBFP2, to assay CRL4 (Cdt2) activity.

APC/C activity is high throughout the tissue, except in a small subset of cells, outlined in yellow. Few cells exhibit PCNA foci, indicating early S Phase, outlined in red.
(Top panel) Mid lobe-region showing oscillations in main cells and (lower panel) distal tip showing oscillations in secondary cells.

C: Endogenous PCNA tagged with GFP in the adult accessory gland shortly post-eclosion. Signal is low in the secondary cells at the distal tip of the lobe which do not endocycle on the day of eclosion.

Scale bars:
A: 50 microns
B,C : 25 microns

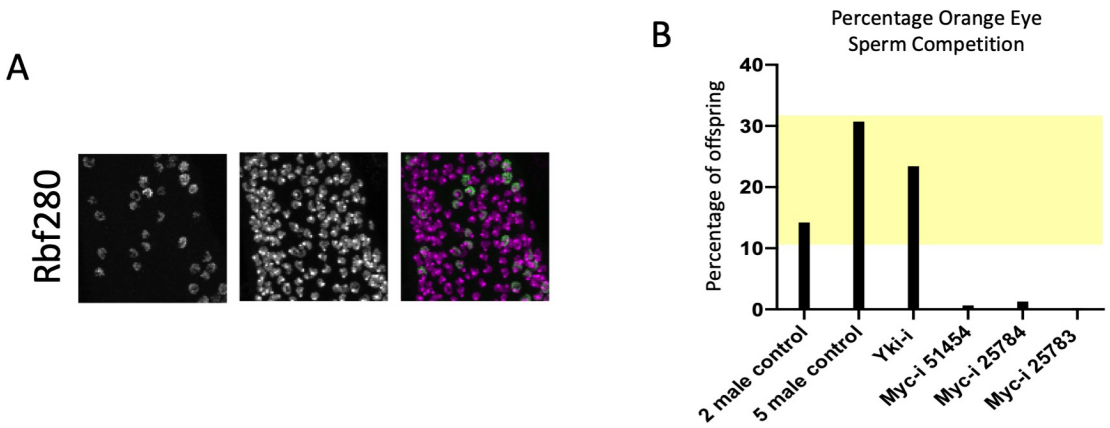

Supplemental Figure 3:

A: EdU incorporation assays in virgin male accessory glands on the day of eclosion. Prd-Gal4 driving UAS-Rbf280 causes increased EdU incorporation in a subset of glands.

B: Quantification of percentage of F1 progeny with red eyes during sperm competition assay for indicated genotypes. Yellow bar represents a normal range of red-eyed progeny when mated with indicated number of control males.

A

DEMISE LINE	Leaky on Eclosion	Recover from Damage
5 - 1	0/4	N/A
9 - 1	3/5	0/8
10 - 2	3/3	3/5

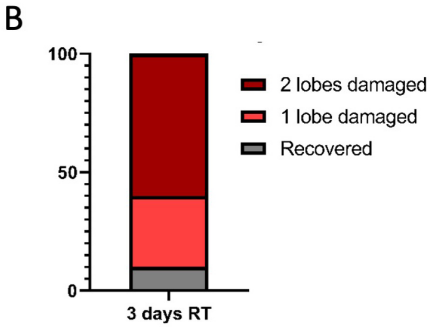

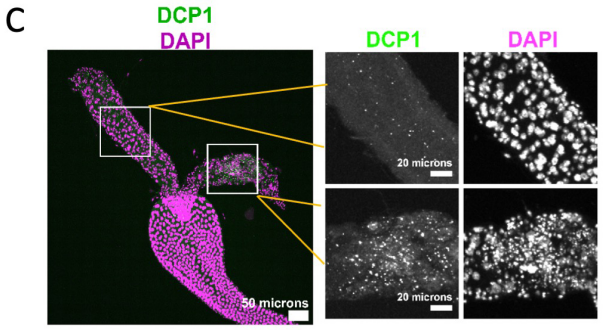

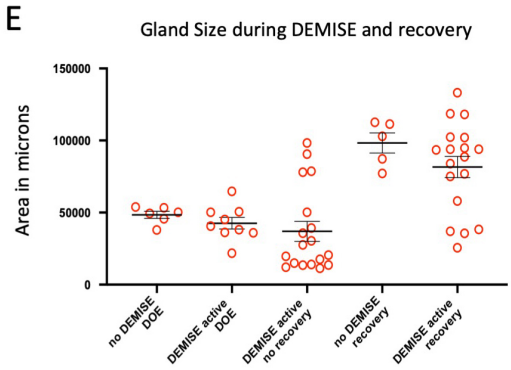

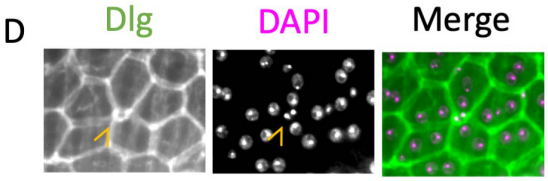

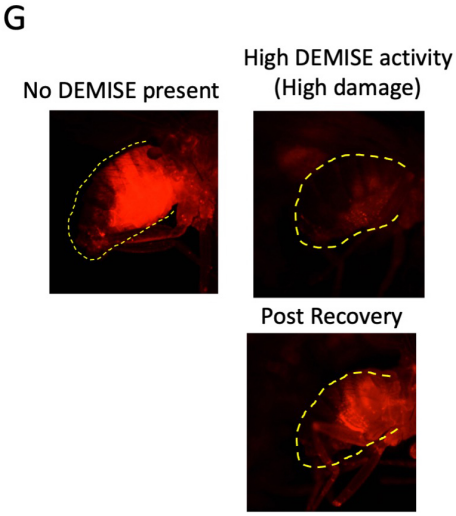

Supplemental Figure 4: DEMISE system

A: Table of additional DEMISE lines screened for use in the adult accessory gland. Lines were scored for leaky expression upon eclosion, whether they were able to induce visible damage

and whether flies recovered at 18°C. Line 5-1 failed to induce damage. Line 9-1 failed to recover at 18°C.

B: Quantification of DEMISE - induced damage and accessory gland phenotypes on day 3 of active DEMISE (kept at room temp): normal size lobes = recovered lobes, 1 damaged lobe, or 2 damaged lobes.

C: DCP1 staining on and accessory gland with DEMISE – induced damage. This representative image shows that the lobe that appears to have more damage has higher levels of DCP1 staining and pyknotic nuclei.

D: DEMISE - induced damage can be visualized as pyknotic nuclei. Yellow arrowhead points to a binucleate accessory gland cell with two pyknotic nuclei showing cell death can occur in the differentiated tissue.

E: Overall gland size quantifications of adult accessory glands. This graph shows data comparing gland size when DEMISE is active and after an 18°C recovery protocol.

F: Prd-Gal4 driving UAS-His2Av::RFP with DEMISE at room temp. Accessory gland fluorescence can be visualized through the abdomen.

G: Representative images of animals using Prd-Gal4 to drive UAS-His2Av::RFP in males with or without DEMISE. Fluorescence is lost in animals undergoing damage and restored (though to a lesser extent than undamaged controls) in animals that have undergone an 18°C recovery protocol.